DOI: 10.61782/fa.2025.0768

FORUM ACUSTICUM
EURONOISE 2025

SHAPE OPTIMISATION FOR THE AEROACOUSTICS, AERODYNAMICS AND HEAT TRANSFER OF ROUND HOLES

Yifei Wang[1*] **Juan Guzmán-Iñigo**[2] **Aimee S. Morgans**[1]

[1] Department of Mechanical, Imperial College London, London, UK.
[2] Department of Engineering, City University of London, London, UK.

ABSTRACT

Acoustic liners are comprised of small holes in the walls of gas turbine combustors. The flow through them both cools the combustion chamber and absorbs acoustic energy, such that their aeroacoustic, aerodynamic, and heat transfer performance are all important. Their circular holes typically have straight edges, whose length (compared to the radius) plays a significant role in their acoustic behaviour. In the case of "short" holes, where the flow through the hole separates without reattaching within it, there can be an amplification of acoustic energy at certain frequencies, leading to a phenomenon known as "whistling". Previous analyses suggests that heat transfer can either exacerbate or mitigate this undesirable occurrence. Furthermore, altering the inlet or outlet geometry of the holes can eliminate the whistling effect, shifting the acoustic behaviour toward damping. Such geometry changes will also affect the holes' aerodynamic and heat transfer performance. This research numerically investigates optimisation of the hole geometry, considering aeroacoustic, aerodynamic performance and heat transfer performance. Simulations integrate the energy equation into a linearised Navier-Stokes solver and employ Bayesian optimisation to refine the orifice shape based on a cost function that combines acoustic absorption, aerodynamic and heat transfer measures. The results indicate that heat transfer through the orifice surface significantly impacts acoustic performance. To enhance the acoustic absorption, a large downstream chamfer is optimal, while for aerodynamics, a moderate upstream chamfer is best. For optimal heat transfer, or to achieve a combined multi-objective target, a large upstream chamfer is identified as the most effective geometry.

Keywords: *Acoustic damping, Optimisation, Holes, Orifices, Acoustic liners, Heat transfer*

1. INTRODUCTION

Thermoacoustic instability occurs when acoustic waves interact with unsteady heat release during combustion. This phenomenon can lead to significant pressure fluctuations within combustors, negatively impacting operational performance and potentially damaging components [1]. The challenge of thermoacoustic instability is especially pertinent when using decarbonised fuels such as hydrogen, with hydrogen flames being especially sensitive to acoustic disturbances due to their high flame speed. Acoustic dampers, like liners and Helmholtz resonators, are often installed in engines to mitigate these issues. These devices absorb acoustic perturbations and help suppress thermoacoustic instability in various industrial applications, including gas turbines and rocket engines.

Acoustic liners consist of multiple circular holes through which a bias flow passes. When the flow travels through these holes, it can significantly enhance the acoustic absorption and effective bandwidth of a perforated liner. Additionally, its tunable properties can be adjusted by varying the mean flow velocity [2]. The mechanism underpinning the acoustic damping is recognised as the conversion of acoustic energy into vortical energy,

*__Corresponding author__: yifei.wang20@imperial.ac.uk.

which is then dissipated as heat [3, 4]. Furthermore, the bias flow from the orifice also provides an impingement jet for cooling the combustor surface [5]. Thus, the effect of heat transfer within the hole must be taken into account.

Howe's model [6] has been widely used to predict the acoustic absorption of holes. It assumes that the hole is infinitely thin and that there is a straight vortex-shedding path from the hole downstream. It predicts that an orifice can absorb sound energy, but cannot generate it. Subsequent research [7] indicates that the dimensions of the orifice significantly impact its acoustic behaviour, and the thickness of the orifice must also be taken into account.

A "short" hole, defined as having a length-to-diameter ratio of less than one but not close to infinitesimal, exhibits flow characteristics that can amplify acoustic energy at certain frequencies, a phenomenon referred to as "whistling" [8–10]. This occurs due to the two-way interaction between acoustic waves and vortical disturbances. It presents challenges in engineering design, as it can decrease the acoustic absorption capability and may even amplify acoustic perturbations, potentially leading to structural failures. The above works considered isothermal hole flows: recent research on heat transferring flows suggests that a temperature gradient can alter the acoustic behaviour of a flow, either increasing or decreasing its acoustic absorption ability [11].

For isothermal hole flows, recent theoretical and numerical studies have shown that the acoustic characteristics of short holes are highly sensitive to their geometry [12,13]. Even minor changes in shape can significantly alter the acoustic response, causing a hole's behaviour to shift from amplification to damping [13, 14]. The present study numerically investigates the optimal performance of short holes, considering aeroacoustic, aerodynamic and heat transfer performance.

2. PROBLEM FORMULATION

2.1 Simulation configuration

To evaluate the aeroacoustic performance, a two-step simulation method is employed [15, 16]. In the first step, the mean flow field is obtained using a Reynolds-Averaged Navier-Stokes (RANS) k-ω-SST turbulence model. Next, acoustic perturbations are added to the mean flow field, which is then solved using a linearised Navier-Stokes Equation (LNSE) solver in the frequency domain. This method has been validated against experimental data and direct simulation techniques, demonstrating greater computational efficiency compared to more intensive methods like Large Eddy Simulation (LES) [13]. Additionally, Bayesian optimisation is utilised as a powerful approach for black-box problems with costly evaluations [17, 18]. The high resource cost associated with each evaluation during the optimisation process limits the number of sampling operations.

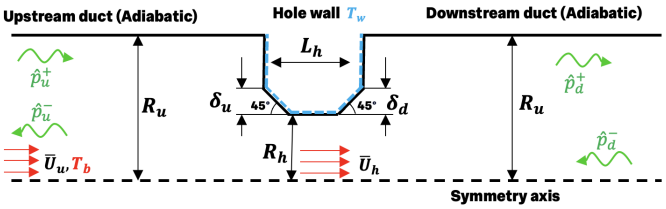

Figure 1. Schematic of the hole configuration, with heat transfer through the wall of the hole.

The configuration studied is a single axisymmetric hole, whose wall is subject to heat transfer. A turbulent mean flow passes through the hole, as illustrated in Figure 1. The radii of the upstream and downstream ducts are R_u, while the radius of the concentric circular hole is R_h. The ratio of the duct radius to the hole radius is $R_u/R_h = 2$. The length of the hole is set to $L_h = 0.66R_h$, which is typical for a short hole. To account for a heat transfer effect, the mean flow is considered to have a temperature of $T_b = 500$ K, while the orifice wall is considered to be at a cooler fixed temperature of $T_w = 300$ K, with the upstream and downstream duct walls considered adiabatic.

A subsonic mean flow with an inlet velocity $\bar{U}_u$ is defined at the inlet boundary as a fully developed turbulent profile. The mean flow is characterised by two dimensionless parameters: the Reynolds number and the Mach number. At the orifice, the Reynolds number is defined as:

$$Re = \frac{R_h \bar{U}_h}{\nu} = 20,000 \tag{1}$$

where $\bar{U}_h$ represents the average flow velocity at the orifice, and ν denotes the kinematic viscosity of the average flow. The Mach number is defined as:

$$M = \frac{\bar{U}_h}{\bar{c}_u} = 0.104 \tag{2}$$

where $\bar{c}_u$ represents the mean speed of sound in the flow. Previous simulations and experimental results [8, 10] suggest a potential for whistling under these flow conditions with a straight hole geometry in adiabatic conditions.

To optimize the geometry, two chamfers are added to the hole edges at both the upstream and downstream sides of the hole. Each edge features a fixed chamfer angle of 45 degrees with variable length, denoted as δ_u for the upstream edge and δ_d for the downstream edge.

The Strouhal number, denoted St, is a dimensionless quantity used to describe normalised frequencies of sound waves. It is defined as:

$$St = fL_h/\bar{U}_h = \frac{\omega}{2\pi} L_h/\bar{U}_h \tag{3}$$

where f is the frequency of the acoustic wave, ω is the angular velocity of the wave and $\bar{U}_h$ represents the mean flow velocity passing through the orifice. In this research, our focus is on Strouhal numbers ranging from 0 to 0.5, as this range is linked to the first whistling mode of the geometry under investigation.

The absorption coefficient, represented as Δ [14, 19, 20], is used as a measure of the aeroacoustic performance of the hole. It is defined as:

$$\Delta = 1 - \frac{|W_u^-| + |W_d^+|}{|W_u^+| + |W_d^-|} \tag{4}$$

where $W_j^{\pm}$ $(j = u, d)$ represents the averaged acoustic energy flux of a plane wave propagating in the positive (+) or negative (-) directions, at the upstream (u) or downstream (d) locations, respectively. It represents the ratio of acoustic energy moving away from the orifice to that entering it. A value of $\Delta = 1$ indicates full absorption, meaning that all incoming energy is absorbed and no acoustic energy escapes the hole. Conversely, $\Delta = 0$ signifies that the acoustic energy remains unchanged by interaction with the hole. If $\Delta < 0$, the acoustic energy is amplified by the presence of the hole, a phenomenon commonly referred to as "whistling".

The aerodynamic characteristics of the orifice are represented by the discharge coefficient, C_d. This is defined as the ratio of the actual discharge to the theoretical discharge from an orifice, expressed as:

$$C_d = \frac{Q_{\text{real}}}{Q_{\text{ideal}}} = \frac{\dot{m}}{A\sqrt{2\rho\Delta P}} \tag{5}$$

where, $\dot{m}$ is the mass flow rate through the hole, A is the cross-sectional area of the hole, ρ is the fluid density, and ΔP is the pressure difference across the hole. Knowing the value of C_d is essential for designing the air distribution system within gas turbine engines [21].

To characterise the heat transfer performance of the hole, we define a normalised power coefficient, denoted P^*, given by:

$$P^* = \frac{P_{wall}}{\rho \bar{U}_h^3 L_{wet}^2} \tag{6}$$

where, P_{wall} represents the power transferred from the orifice wall to the flow. The sign of P_{wall} indicates the direction of heat transfer: a positive value means that the wall loses heat to the flow, while a negative value indicates that the wall absorbs heat from the flow. The denominator, $\rho \bar{U}_h^3 L_{wet}^2$, represents the kinetic power of the flow and has units of Watts. ρ is the mean flow density, $\bar{U}_h$ is the mean flow velocity, and L_{wet} refers to the total length of the orifice wall, which includes the hole length, chamfer length, and radial length in cross-section. The coefficient P^* quantifies the ratio between the energy transferred into the flow and the flow kinetic energy through the hole.

2.2 Numerical Implementation

To evaluate all of the aerodynamic, heat transfer and aeroacoustic performance, a two-step simulation method was employed [15, 16] which decomposed the fluid variables into mean and perturbation terms. The first step involved obtaining the mean turbulent flow field using a compressible Reynolds-Averaged Navier-Stokes (RANS) simulation with the open-source solver OpenFoam (version 11). A steady-state simulation solution was achieved using the SIMPLE algorithm along with the K-Omega SST turbulence model. A fully developed turbulent flow profile was imposed at the inlet boundary, where the inlet pressure was defined as a zero gradient, and the outlet pressure was set to zero gauge pressure. The temperature of the flow inlet is assigned $T = 500$ K. The upstream and downstream walls are set to adiabatic and the hole wall is set to a fixed temperature T_{wall} = 300 K. The upstream, downstream, and wall surfaces were assigned a no-slip condition.

The second step then involved solving for the linearised flow perturbations using a compressible linearised Navier-Stokes Equation (LNSE) solver. This was performed in the frequency domain using a finite element method within the open-source computing framework FEniCS [22], with more detail provided in [23]. Non-reflecting boundary conditions were implemented at both the inlet and outlet boundaries, and acoustic waves of different frequencies were forced from the inlet boundary into the downstream flow. The acoustic response was evaluated using the two-microphone method at the inlet and outlet boundaries to distinguish between the acoustic waves. For the acoustic perturbations, the walls of the hole

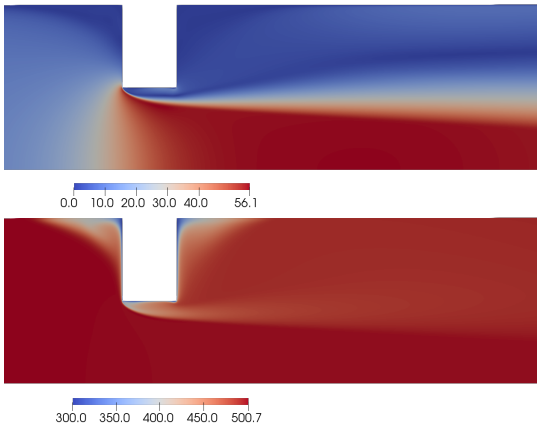

Figure 2. Magnitude of the mean flow velocity field (upper) and temperature field (lower) for the original, unmodified hole geometry with a wall temperature $T_{wall} = 300K$.

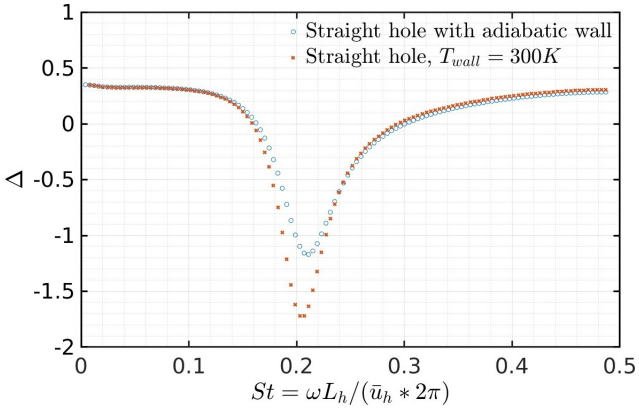

Figure 3. Absorption coefficient Δ of original geometry with an adiabatic wall and with a cooler wall. Negative Δ indicates the acoustic amplifying phenomenon known as "whistling".

were defined as non-slip boundaries with $\hat{\mathbf{u}} = 0$. The upstream and downstream walls were assigned slip boundary conditions $\hat{\mathbf{u}} \cdot \mathbf{n} = 0$ to reduce the computational costs that would be associated with acoustic boundary layers along the upstream and downstream duct walls.

For isothermal flows, the two-step method was validated for straight holes against experimental data and direct simulation techniques, demonstrating accuracy and computational efficiency [13]. For the present work, validation was for the isothermal straight hole geometry, with the $u_d, u_u = 0$, condition validated by comparison to experimental data and numerical simulations [23]. The mean velocity and temperature fields of the straight hole (δ_u, δ_d = 0) with $T_{wall} = 300K$ are shown in Figure 2. This mean flow field is subsequently used in the perturbation solver to determine the acoustic response to an input acoustic wave. The absorption coefficient Δ as a function of frequency St is shown in Figure 3.

2.3 Optimisation configuration

The geometry of a straight hole serves as the baseline for optimizing the aeroacoustic, aerodynamic, and heat transfer performance. With the acoustic performance known to be sensitive to geometry [13], two 45-degree chamfers of variable length were added to the upstream (inlet) and downstream (outlet) edges of the hole to modify the energy amplification. The optimisation algorithm controls the depths of the two chamfers, δ_u,δ_d, while keeping the total length of the hole constant ($\delta_u + \delta_d < L_h$).

For the optimisation procedure, Bayesian optimisation was chosen, this being a powerful approach for black-box problems with costly evaluations [17, 18]. For the present numerical problem, computing the mean flow solution and perturbations at a single frequency takes approximately 500 CPU hours, primarily due to the mean flow simulation. Bayesian optimisation is performed using a modified version of the scikit-optimize library that includes a constraint function [24] [25]. The acquisition function is set to the probability of improvement (EI), and the acquisition optimizer function is configured as "lbfgs." The optimisation problem is formulated as follows:

$$\arg\max_{\delta_u, \delta_d} f(\delta_u, \delta_d) \tag{7}$$

subject to $\delta_u \in [0, L_h]$, $\delta_d \in [0, L_h]$ and $\delta_u + \delta_d \leq L_h$ to maintain the geometry's topology. 45 initial sampling points, selected using the grid method, were computed in advance to initiate the optimisation. The optimisation was performed for 5 steps to provide a fast indication of the potential optimal geometry.

The acoustic absorption coefficient, Δ, of a straight hole with and without heat transfer is shown in Figure 3. Δ shows acoustic energy amplification in the frequency range $0.16 < St < 0.30$, with the most pronounced whistling effect occurring at $St = 0.20$, for which Δ reaches its minimum value of -1.72. The presence of a hot bias flow and heat transfer increased the maximum nega-

tive value of Δ; this is consistent with recent research [11] suggesting that heat transfer out of a flow can increase Δ and vice versa.

In this study, the acoustic absorption coefficient at frequency $St = 0.20$, denoted $\Delta_{st=0.20}$, is identified as the aeroacoustic parameter that needs optimisation. The aerodynamic performance is represented by the discharge coefficient, C_d, and the heat transfer performance by the normalised heat transfer power, $P*$, both of which depend only on the mean flow solution. The values of these three performance parameters for the straight (unmodified) hole are summarised in Table 1.

Table 1. Aeroacoustic, aerodynamic and heat transfer performance of unmodified straight hole geometry.

Geometry	$\Delta_{st=0.20}$	C_d	$\lvert P^* \rvert$
$\delta_u, \delta_d = 0$	-1.72	0.66	0.77

In order to perform an optimisation which accounts for aeroacoustic, aerodynamic and heat transfer performance, an objective function f is defined which combines all three using weighting factors α, β and γ:

$$f = \alpha\,\Delta_{st=0.20} + \beta\,C_d + \gamma|P^*| \tag{8}$$

By altering these weight factors such that they sum to unity, optimal geometries can be obtained which differently prioritise the three performances.

3. RESULTS

3.1 Optimisation of only the acoustic absorption coefficient $\Delta_{st=0.20}$

When optimisation is performed for solely the aeroacoustic performance (i.e. $\alpha = 1$, $\beta = 0$, $\gamma = 0$), the results in Figure 4 show that an orifice with a large downstream chamfer would provide the best aeroacoustic absorption performance. The mechanism of the improved performance is likely to be associated with the downstream edge being moved further from the vortex shedding path, weakening the generation of acoustic waves at the hole opening.

3.2 Optimisation of only the aerodynamic performance, C_d

When optimisation is performed for solely the aerodynamic performance (i.e. $\alpha = 0$, $\beta = 1$, $\gamma = 0$),

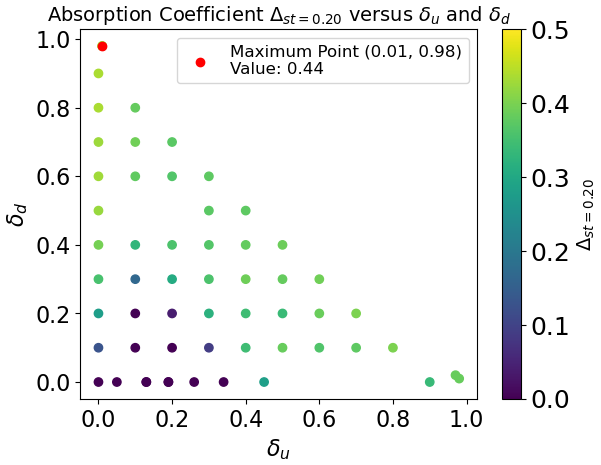

Figure 4. Acoustic absorption coefficient $\Delta_{st=0.20}$ versus δ_u and δ_d. An optimised value of $\Delta_{st=0.20} = 0.44$ was found for which $\delta_u = 0.01L_h$ and $\delta_d = 0.98L_h$.

the optimisation results in Figure 5 show that a moderate upstream chamfer of size $\delta_u = 0.19L_h$ and no downstream chamfer($\delta_d = 0$) is best. The presence of an upstream chamfer reduces flow separation at the upstream edge, which ultimately helps to alleviate the pressure drop across the hole.

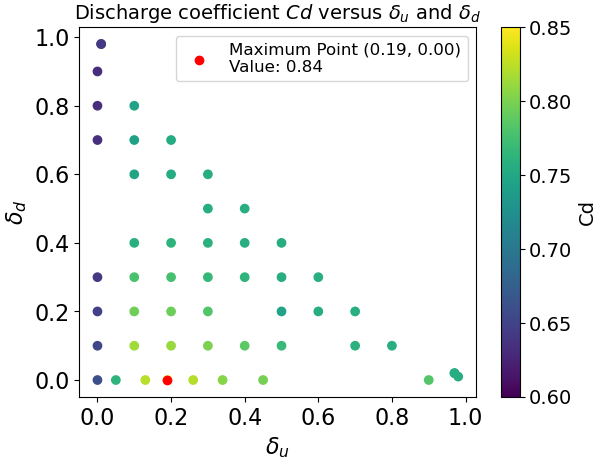

Figure 5. Discharge coefficient C_d versus δ_u and δ_d. An optimised value of $C_d = 0.84$, was found for which $\delta_u = 0.19L_h$ and $\delta_d = 0.0$.

3.3 Optimisation of only the heat transfer performance, $|P*|$

When optimisation is performed for solely the heat transfer performance (i.e. $\alpha = 0$, $\beta = 0$, $\gamma = 1$), the optimisation results in Figure 6 show that a large upstream chamfer provides the highest heat transfer. This outcome can be attributed to the larger contact area created with the flow upstream, which enhances heat transfer.

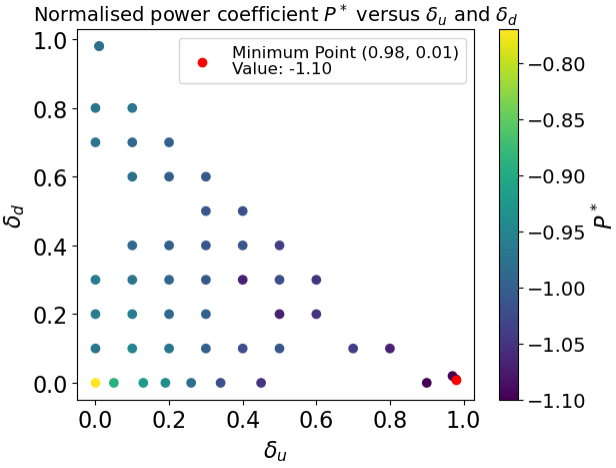

Figure 6. Normalised power coefficient P^* versus δ_u and δ_d, with the highest heat transfer performance obtained for $\delta_u = 0.98L_h, \delta_d = 0.01L_h$

3.4 Optimisation for combined objective function

For the multi-objective optimisation, the combined objective function in Equation 8, is applied using weight factors of $\alpha = 0.33$, $\beta = 0.33$, and $\gamma = 0.33$. With this combination of weight factors, the optimisation process returns an optimal geometry characterised by a large upstream chamfer, consistent with the results of P^*. This results in a high heat transfer power transfer coefficient while causing only minor reductions (compared to the best achievable) in $\Delta_{st=0.20}$ and C_d. A summary of these geometries is presented in Table 2. The aeroacoustic performance of the optimized geometry is illustrated in Figure 3, while the mean flow fields are depicted in Figure 2.

4. CONCLUSION

The present work has presented a two-step simulation method for simultaneously characterising the aeroacous-

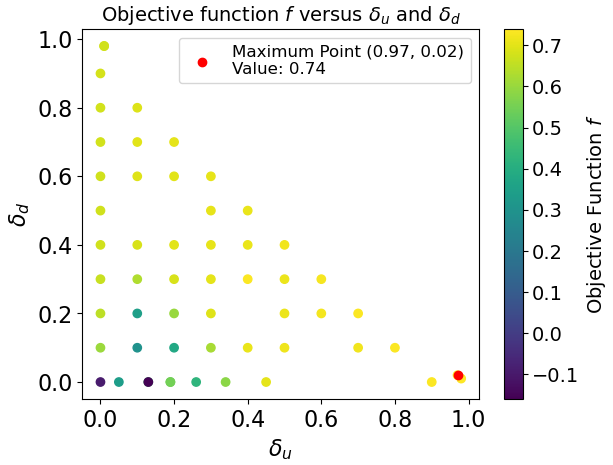

Figure 7. The combined cost function f, which accounts for aeroacoustic, aerodynamic, and heat transfer performance, δ_u and δ_d.

Table 2. Summary of the performance of the original and optimised geometries.

Geometry(δ_u, δ_d)	$\Delta_{st=0.20}$	C_d	$\lvert P^* \rvert$	f
Straight(0,0)	-1.72	0.66	0.77	-0.09
$(0.01L_h, 0.98L_h)$	0.43	0.64	0.98	0.68
$(0.19L_h, 0)$	-0.17	0.86	0.97	0.55
$(0.98L_h, 0.01L_h)$	0.38	0 .76	1.10	0.74

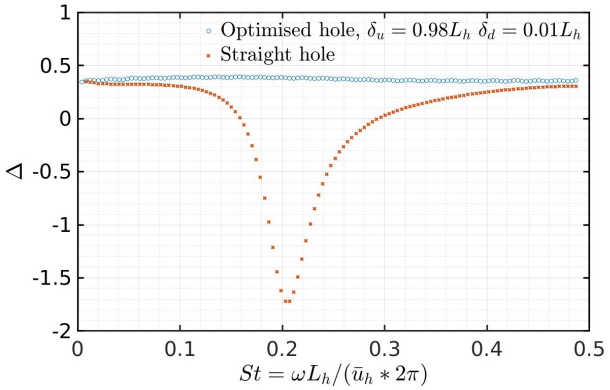

Figure 8. Absorption coefficient Δ of original straight geometry and optimised geometry under objective function f.

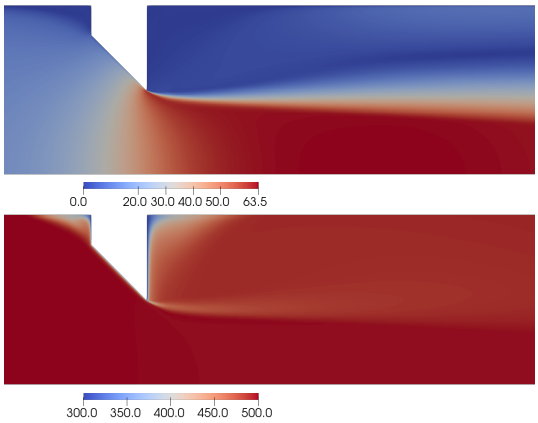

Figure 9. Magnitude of the mean flow velocity field (upper) and temperature field (lower) for the optimised hole.

tic, aerodynamic and heat transfer performance of a hole flow with heat transfer. Heat transfer through the wall of the hole is seen to accentuate the acoustic whistling effect in the absence of hole geometry changes. A Bayesian optimisation technique for optimising the chamfer lengths of 45 degree chamfers at both the hole inlet and hole outlet was then employed.

The optimisation can target the individual aeroacoustic, aerodynamic, and heat transfer performances resulting in three distinct optimal geometries. It was also shown that it is possible to apply a combined objective function which incorporates different combinations of the above three performance measures. The optimal geometry then obtained involves a large upstream chamfer which ensures good heat transfer, aerodynamic and aeroacoustic performance.

This work thus represents a step in being able to design the shapes of orifices according to acoustic, aerodynamic and heat transfer priorities, with finer geometry control being possible through additive manufacturing.

5. REFERENCES

[1] A. S. Morgans and D. Yang, "Thermoacoustic instability in combustors," *Annual Review of Fluid Mechanics*, vol. 57, pp. 9–33, 2025.

[2] X. Jing and X. Sun, "Experimental investigations of perforated liners with bias flow," *The Journal of the Acoustical Society of America*, vol. 106, p. 2436–2441, 1999.

[3] J. D. Eldredge and A. P. Dowling, "The absorption of axial acoustic waves by a perforated liner with bias flow," *Journal of Fluid Mechanics*, vol. 485, pp. 307–335, 2003.

[4] I. J. Hughes and A. P. Dowling, "The absorption of sound by perforated linings," *Journal of Fluid Mechanics*, vol. 218, pp. 299–335, 1990.

[5] J. G. von Saldern, M. E. Eck, J. P. Beuth, B. Ćosić, and K. Oberleithner, "Acoustic characteristics of impingement cooling sheets; effect of bias-grazing flow interaction on the liner impedance in a thin annulus," *Journal of Sound and Vibration*, vol. 527, p. 116818, 2022. Available online 18 February 2022, © 2022 Elsevier Ltd. All rights reserved.

[6] M. Howe, "On the theory of unsteady high reynolds number flow through a circular aperture," *Proc. R. Soc. A*, vol. 366, no. 1725, pp. 205–23, 1979.

[7] X. Jing and X. Sun, "Effect of plate thickness on impedance of perforated plates with bias flow," *AIAA Journal*, vol. 38, no. 9, 2000.

[8] P. Testud, Y. Aurégan, P. Moussou, and A. Hirschberg, "The whistling potentiality of an orifice in a confined flow using an energetic criterion," *Journal of Sound and Vibration*, vol. 325, pp. 769–780, Sept. 2009.

[9] J. Su, J. Rupp, A. Garmory, and J. F. Carrotte, "Measurements and computational fluid dynamics predictions of the acoustic impedance of orifices," *Journal of Sound and Vibration*, vol. 352, p. 174–191, 2015.

[10] R. Lacombe, S. Föll, G. Jasor, W. Polifke, Y. Aurégan, and P. Moussou, "Identification of aero-acoustic scattering matrices from large eddy simulation: application to whistling orifices in duct," *Journal of Sound and Vibration*, vol. 332, pp. 5059–5067, 2013.

[11] S. R. Yeddula, R. Gaudron, and A. S. Morgans, "Acoustic absorption and generation in ducts of smoothly varying area sustaining a mean flow and a mean temperature gradient," *Journal of Sound and Vibration*, vol. 515, p. 116437, sep 2021. Available online 16 September 2021.

[12] D. Yang and A. S. Morgans, "Asemi-analytical model for the acoustic impedance of finite length circular holes with mean flow," *Journal of Sound and Vibration*, vol. 384, p. 294–311, 2016.

[13] J. Guzmán-Iñigo, D. Yang, H. G. Johnson, and A. S. Morgans, "Sensitivity of the acoustics of short circular holes with bias flow to inlet edge geometries," *AIAA Journal*, vol. 57, no. 11, pp. 4835–4844, 2019.

[14] J. Guzmán-Iñigo and A. S. Morgans, "Designing the edges of holes(with bias flow) to maximise acoustic damping," *Journal of Sound and Vibration*, vol. 575, no. 11, p. 118224, 2024.

[15] A. Kierkegaard, S. Boij, and G. Efraimsson, "A frequency domain linearized navier–stokes equations approach to acoustic propagation in flow ducts with sharp edges," *The Journal of the Acoustical Society of America*, vol. 127, pp. 710–719, 2010.

[16] J. Guzmán-Iñigo and A. S. Morgans, "Influence of the shape of a short circular hole with bias flow on its acoustic response," in *28th AIAA/CEAS Aeroacoustics Conference*, (Southampton, UK), June 2022.

[17] B. Shahriari, K. Swersky, Z. Wang, R. P. Adams, and N. de Freitas, "Taking the human out of the loop: A review of bayesian optimization.," *Proceedings of the IEEE*, vol. 104, no. 1, p. 148–175, 2016.

[18] M. T. Morar, *Bayesian Optimisation over Mixed Parameter Spaces*. PhD thesis, University of Manchester, Manchester, United Kingdom, 2021. Doctoral Dissertation. Engineering and Physical Sciences. https://pure.manchester.ac.uk/ws/portalfiles/portal/194689010/FULL_TEXT.PDF.

[19] R. Gaudron, J. Guzmán Iñigo, and A. S. Morgans, "Variation of acoustic energy across sudden area expansions sustaining a subsonic flow," *AIAA Journal*, vol. 6, no. 1, 2023.

[20] I. D. J. Dupere and A. P. Dowling, "The use of helmholtz resonators in a practical combustor," *Journal of engineering for gas turbines and power*, vol. 127, no. 2, p. 268–275, 2005.

[21] N. Hay and A. Spencer, "Discharge coefficients of cooling holes with radiused and chamfered inlets," *Journal of Turbomachinery*, vol. 114, no. 4, p. 701–706, 1992.

[22] M. S. Alnæs, J. Blechta, J. Hake, A. Johansson, B. Kehlet, A. Logg, C. Richardson, J. Ring, M. E. Rognes, and G. N. Wells, "The FEniCS project version 1.5," *Archive of Numerical Software*, vol. 3, no. 100, pp. 9–23, 2015. Received: May 28, 2015; Final revision: December 1, 2015; Published: December 7, 2015.

[23] J. Guzmán-Iñigo, D. Yang, R. Gaudron, and A. S. Morgans, "On the scattering of entropy waves at sudden area expansions," *Journal of Sound and Vibration*, vol. 540, p. 117261, 2022.

[24] scikit-optimize developers, "scikit-optimize: Sequential model-based optimization in python," 2021.

[25] S. Torbati, A. Daneshmehr, H. Pouraliakbar, M. Asgharian, S. H. Ahmadi Tafti, D. Shum-Tim, *et al.*, "Personalized evaluation of the passive myocardium in ischemic cardiomyopathy via computational modeling using Bayesian optimization," *Biomech. Model. Mechanobiol.*, 2024. Available online 2024.